

## Monodisperse Nickel Nanoparticles and Their Catalysis in Hydrolytic Dehydrogenation of Ammonia Borane

Önder Metin,<sup>†,‡</sup> Vismadeb Mazumder,<sup>†</sup> Saim Özkar,<sup>‡</sup> and Shouheng Sun<sup>\*†</sup>

Department of Chemistry, Brown University, Providence, Rhode Island 02912, and Department of Chemistry, Middle East Technical University, 06531, Ankara, Turkey

Received October 30, 2009; E-mail: ssun@brown.edu

Hydrogen has been considered as one of the best alternative energy carriers to satisfy the increasing demand for an efficient and clean energy supply.<sup>1</sup> Controlled storage and release of hydrogen are the widely known technological barriers in the fuel cell based hydrogen economy.<sup>2,3</sup> Recently, the ammonia–borane (AB, H<sub>3</sub>NBH<sub>3</sub>) complex was identified as one of the leading candidates as a hydrogen reservoir owing to its high hydrogen content (19.6 wt %), high stability under ordinary fuel cell reaction conditions, and nontoxicity.<sup>4</sup> Hydrogen stored in the AB complex can be released through either pyrolysis or hydrolysis. The pyrolysis of AB shows the release of only 6.5 wt % of H<sub>2</sub> at 85 °C, and the release of more hydrogen from AB requires much higher temperatures.<sup>5</sup> In contrast, the hydrolysis of AB in the presence of a suitable catalyst provides 3 mol of hydrogen per mol of AB at room temperature.<sup>6</sup> Among the catalyst systems tested thus far,<sup>7</sup> platinum has shown the highest activity in this hydrolysis reaction.<sup>8</sup> However, the concerns over the practical usage of platinum have motivated the search for a low cost catalyst for the same hydrolysis reaction. In this regard, the preparation of a non-noble metal catalyst with a high hydrolysis activity is clearly a desired goal.

Here we report a facile synthesis of monodisperse nickel (Ni) nanoparticles (NPs) and their active catalysis for H<sub>2</sub> release from the hydrolysis of AB at ambient conditions. The Ni NPs have attracted much attention due to their activity in catalyzing AB hydrolysis.<sup>9</sup> Various solution-phase synthetic methods have been developed to prepare Ni NPs, and monodisperse Ni NPs are normally made by decomposition of Ni complexes in the presence of surfactants that bind strongly to Ni.<sup>10</sup> Ni NPs protected by such a robust coating are not active catalysts, and high temperature treatments used to activate Ni NP catalyst often cause inevitably NP aggregation and catalysis deterioration. Recently, we demonstrated that monodisperse Au or Pd NPs can be synthesized by the reduction of HAuCl<sub>4</sub> or Pd(acac)<sub>2</sub> (acac = acetylacetonate) with borane tributylamine (BTB) complex in the presence of oleylamine (OAm).<sup>11,12</sup> OAm acted as a surfactant, and both of the sub-10 nm NPs were found to be better electrocatalysts than commercially available materials for oxygen reduction reaction<sup>13</sup> or formic acid oxidation.<sup>12</sup> Our improved synthesis indicated that monodisperse Ni NPs could also be made by reducing Ni(acac)<sub>2</sub> with BTB. The catalytic experiments showed that, without any special treatment to remove the surfactants, the as-synthesized Ni NPs exhibited high catalytic activity for the hydrolysis of the AB complex with a total turnover frequency (TOF) value of 8.8 mol of H<sub>2</sub>·(mol of Ni)<sup>-1</sup>·min<sup>-1</sup>, the best among all the nickel catalysts ever reported.

The monodisperse Ni NPs were formed from the reduction of Ni(acac)<sub>2</sub> with BTB in OAm and oleic acid (OA). In the reaction, OAm was used as both a solvent and surfactant, BTB served as a

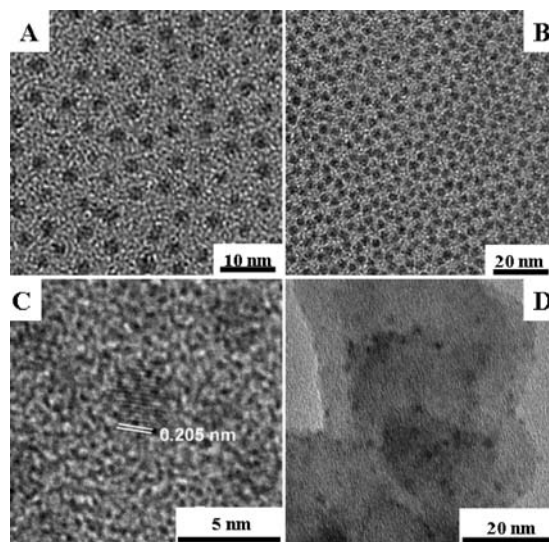


**Figure 1.** TEM images of (A) the 3.2 nm Ni NPs, (B) a double layer array of the 3.2 nm Ni NPs, (C) the 3.2 nm Ni NP with (111) lattice fringe distance indicated, and (D) the 3.2 nm Ni NPs deposited on Ketjen carbon support.

reducing agent, and OA was added as a cosurfactant for Ni NP stabilization.<sup>14</sup> Figure 1A shows a transmission electron microscopy (TEM) image of the 3.2 nm Ni NPs from the hexane dispersion. The NPs have a standard deviation of ~7% in the diameter. Figure 1B is the TEM image of a double layer array of the 3.2 nm Ni NPs. The small Ni NPs on the second layer tend to occupy the saddle point between two Ni NPs in the first monolayer assembly, inconsistent with what has been observed in the small Au, FePt, and PbSe NPs.<sup>15</sup> A high-resolution TEM (HRTEM) study of a series of single Ni NPs indicate that the as-synthesized Ni NPs have a polycrystalline structure (Figure 1C) but the (111) planes can still be identified by the typical interfringe distance of 0.205 nm, which is close to the lattice spacing of the (111) planes of the face-centered cubic (fcc) Ni crystal (0.203 nm). The polycrystalline nature of the Ni NPs is confirmed by their broad X-ray diffraction pattern (Figure S1).

Of the two Ni precursors [Ni(acac)<sub>2</sub> and Ni(acetate)<sub>2</sub>] tested under the current synthetic conditions, Ni(acac)<sub>2</sub> empirically gave the better quality Ni NPs (Figure S2). The use of OA was the key to obtain monodisperse Ni NPs. Without OA, polydisperse Ni NPs were obtained, but the XRD pattern shows that such polydisperse NPs have a better fcc-Ni crystal structure (Figure S3). Although 3.2, 4.2, and 5.4 nm Ni NPs could be obtained by varying the molar ratio of BTB/Ni = 3, 2 and 1, respectively, the current synthetic conditions could not tune the NP size well. Larger Ni NPs did not show as narrow a size distribution as that in the 3.2 nm size range (Figure S4), indicating that more BTB facilitates uniform Ni

<sup>†</sup> Brown University.

<sup>‡</sup> Middle East Technical University.

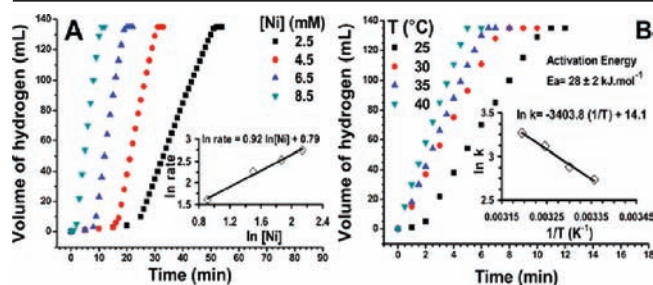


**Figure 2.** Plots of volume of hydrogen generated vs time. (A) The hydrolysis of AB was catalyzed by the 3.2 nm Ni/C catalyst at different catalyst concentrations ( $[AB] = 200$  mM,  $T = 25 \pm 1$  °C) (inset:  $\ln [\text{rate}]$  vs  $\ln [\text{Ni}]$ ) and (B) the catalysis was studied at different temperatures in the range 25–40 °C ( $[\text{Ni}] = 8.5$  mM,  $[AB] = 200$  mM) (inset: Arrhenius plot ( $\ln k$  vs  $1/T$ )).

nucleation and growth. Elemental analyses revealed that the 3.2 nm Ni NPs showed no boron contamination and they contained 22 wt % of Ni.

The catalytic activity of the 3.2 nm Ni NPs toward hydrolytic dehydrogenation of the AB complex was evaluated in a typical water-filled graduated buret system.<sup>14</sup> The 3.2 nm Ni NPs were supported on Ketjen carbon (surface area 800 m<sup>2</sup>/g) and employed as catalyst without any further treatment.<sup>14</sup> The TEM image of the 3.2 nm Ni/C catalyst (Figure 1D) shows that Ni NPs preserve their size after dispersion over the carbon support. Figure 2A shows a plot of the hydrogen generated versus time during the catalytic hydrolysis of AB at different catalyst concentrations. It can be seen that there exists an initiation process in the first catalytic cycle for the NP catalyst in hydrogen generation and the time needed to activate the NP catalyst is dependent on the catalyst concentration; the higher the catalyst or substrate concentration, the shorter the initiation period. After this initiation process, a rapid and almost linear hydrogen evolution is observed. A stoichiometric amount of hydrogen ( $\sim 3$  mmol of H<sub>2</sub>) is generated in less than 20 min. The inset in Figure 2A shows the plot of hydrogen generation rate versus Ni concentration on a logarithmic scale. A slope of 0.92–1.00 in the inset indicates that the hydrolysis catalyzed by the 3.2 nm Ni/C catalyst is first-order in catalyst concentration but zero-order in AB concentration (Figure S5). An acid–base titration test<sup>14</sup> showed that there was no detectable amount of ammonia gas formed during the AB dehydrogenation process, indicating that the gas generated during the reaction is nearly pure H<sub>2</sub> which is very important for fuel cell applications.<sup>16</sup>

Figure 2B shows the volume of hydrogen generated versus time during the catalytic hydrolysis of AB at various temperatures in the range 25–40 °C. The rate constant  $k$ 's at different temperatures were calculated from the slope of the linear part of each plot in Figure 2B. The inset of Figure 2B shows the Arrhenius plot ( $\ln k$  vs  $1/T$ ), from which the activation energy for the hydrolytic dehydrogenation is calculated to be  $28 \pm 2$  kJ·mol<sup>-1</sup>. Activities in terms of TOF values (mol of H<sub>2</sub>·(mol of catalyst·min)<sup>-1</sup>) of previously reported nickel catalysts, which have been tested in the hydrolysis of AB, are given in Table S1. Our 3.2 nm Ni/C catalyst has the highest activity among all the nickel catalysts studied. The enhanced activity of our catalyst stems from the small size and monodispersity of the particles, leading to a better dispersion on the carbon support.<sup>17</sup> A reusability test shows that the 3.2 nm Ni/C

catalyst retains  $\sim 80\%$  of its initial activity after the fifth cycle (Figure S6). The small activity loss may be due to agglomeration. Nevertheless, the 3.2 nm Ni/C catalyst provides 4261 turnovers over 23 h in the hydrolysis of AB at  $25 \pm 1$  °C.

In summary, we have reported a facile synthesis of monodisperse Ni NPs by the reduction of Ni(acac)<sub>2</sub> with BTB in the presence of OAm and OA. The Ni NPs supported on Ketjen carbon are highly active for hydrolytic dehydrogenation of the AB complex even at low catalyst and substrate concentrations at room temperature. Such Ni NP based catalysis under mild reaction conditions represents a promising step toward the practical development of the AB complex as a feasible hydrogen storage medium for fuel cell applications.

**Acknowledgment.** Ö.M. thanks TUBITAK for 2214-Research fellowship program and the METU-DPT-OYP program on the behalf of Ataturk University.

**Supporting Information Available:** Synthesis and characterization of Ni NPs and the kinetics of hydrogen generation from the hydrolysis of AB. This material is available free of charge via the Internet at <http://pubs.acs.org>.

## References

- Schlapbach, L.; Züttel, A. *Nature* **2001**, *414*, 353–358.
- Basic Research Needs for the Hydrogen Economy. Report of the Basic Energy Sciences Workshop on Hydrogen Production, Storage and Use, May 13–15, 2003, Office of Science, U.S. Department of Energy, <http://www.sc.doe.gov/bes/hydrogen.pdf>.
- Züttel, A. *Mater. Today* **2003**, *6*, 24.
- (a) Marder, T. B. *Angew. Chem., Int. Ed.* **2007**, *46*, 8116. (b) Stephens, F. H.; Pons, V.; Baker, R. T. *Dalton Trans* **2007**, *25*, 2613, and references therein.
- (a) Baitalow, F.; Baumann, J.; Wolf, G.; Jaenicke, K.; Leitner, G. *Thermochim. Acta* **2002**, *391*, 159. (b) Wolf, G.; Baumann, J.; Baitalow, F.; Hoffman, F. P. *Thermochim. Acta* **2000**, *343*, 19.
- Chandra, M.; Xu, Q. *J. Power Sources* **2006**, *156*, 190.
- (a) Cheng, F.; Ma, H.; Li, Y.; Chen, J. *Inorg. Chem.* **2007**, *46*, 788. (b) Clark, T. J.; Whittell, G. R.; Manners, I. *Inorg. Chem.* **2007**, *46*, 7522. (c) Kalidindi, S. D.; Sayal, U.; Jagirdar, B. R. *Phys. Chem. Chem. Phys.* **2008**, *10*, 5870. (d) Yan, J. M.; Zhang, X. B.; Han, S.; Shioyama, H.; Xu, Q. *Angew. Chem., Int. Ed.* **2008**, *47*, 2287. (e) Metin, Ö.; Özkar, S. *Energy Fuels* **2009**, *23*, 3517. (f) Metin, Ö.; Sahin, S.; Özkar, S. *Int. J. Hydrogen Energy* **2009**, *34*, 6304. (g) Yan, J.-M.; Zhang, X.-B.; Shioyama, H.; Xu, Q. *J. Power Sources* **2010**, *195*, 1091.
- (a) Chandra, M.; Xu, Q. *J. Power Sources* **2006**, *159*, 855. (b) Chandra, M.; Xu, Q. *J. Power Sources* **2007**, *168*, 135.
- (a) Chandra, M.; Xu, Q. *J. Power Sources* **2006**, *163*, 364. (b) Kalidindi, S. D.; Indirani, M.; Jagirdar, B. R. *Inorg. Chem.* **2008**, *47*, 7424. (c) Yao, C. F.; Zhuang, L.; Cao, Y. L.; Ai, X. P.; Yang, H. X. *Int. J. Hydrogen Energy* **2008**, *33*, 2462. (d) Yan, J.-M.; Zhang, X.-B.; Han, S.; Shioyama, H.; Xu, Q. *Inorg. Chem.* **2009**, *48*, 7389. (e) Umegaki, T.; Yan, J.-M.; Zhang, X.-B.; Shioyama, H.; Kuriyama, N.; Xu, Q. *Int. J. Hydrogen Energy* **2009**, *34*, 3816. (f) Umegaki, T.; Yan, J.-M.; Zhang, X.-B.; Shioyama, H.; Kuriyama, N.; Xu, Q. *J. Power Sources* **2009**, *191*, 209. (g) Yan, J.-M.; Zhang, X.-B.; Han, S.; Shioyama, H.; Xu, Q. *J. Power Sources* **2009**, *194*, 478. (h) Kalidindi, S. B.; Sanyal, U.; Jagirdar, B. R. *Phys. Chem. Chem. Phys.* **2008**, *10*, 5870.
- (a) Bradley, J. S.; Tesche, B.; Busser, W.; Maase, M.; Reetz, M. T. *J. Am. Chem. Soc.* **2000**, *122*, 4631. (b) Murray, C. B.; Sun, S.; Doyle, H.; Betley, T. *MRS Bull.* **2001**, *26*, 985. (c) Park, J.; Kang, E.; Son, S. U.; Park, H. M.; Lee, M. K.; Kim, J.; Kim, K. W.; Noh, H.-J.; Park, J.-H.; Bae, C. J.; Park, J.-G.; Hyeon, T. *Adv. Mater.* **2005**, *17*, 429. (d) Wang, H.; Jiao, X.; Chen, D. J. *Phys. Chem. C* **2008**, *112*, 18793.
- Peng, S.; Lee, Y.; Wang, C.; Yin, H.; Dai, S.; Sun, S. *Nano Res.* **2008**, *1*, 229.
- Mazumder, V.; Sun, S. *J. Am. Chem. Soc.* **2009**, *131*, 4588.
- Lee, Y.; Loew, A.; Sun, S. *Chem. Mater.* **2009**, ASAP, doi: 10.1021/cm9013046.
- See the Supporting Information.
- (a) Shevchenko, E. V.; Talapin, D. V.; Murray, C. B.; O'Brien, S. *J. Am. Chem. Soc.* **2006**, *128*, 3620. (b) Kim, J.; Rong, C.; Liu, J. P.; Sun, S. *Adv. Mater.* **2009**, *21*, 906.
- Ramachandran, P. V.; Gagare, P. D. *Inorg. Chem.* **2007**, *46*, 7810.
- Pina, G.; Louis, C.; Keane, M. A. *Phys. Chem. Chem. Phys.* **2003**, *5*, 1924.

JA909243Z